



HAL
open science

Seasonality and extent of extratropical TST derived from in-situ CO measurements during SPURT

P. Hoor, C. Gurk, D. Brunner, M. I. Hegglin, H. Wernli, H. Fischer

► **To cite this version:**

P. Hoor, C. Gurk, D. Brunner, M. I. Hegglin, H. Wernli, et al.. Seasonality and extent of extratropical TST derived from in-situ CO measurements during SPURT. *Atmospheric Chemistry and Physics Discussions*, 2004, 4 (2), pp.1691-1726. hal-00301166

HAL Id: hal-00301166

<https://hal.science/hal-00301166>

Submitted on 18 Jun 2008

HAL is a multi-disciplinary open access archive for the deposit and dissemination of scientific research documents, whether they are published or not. The documents may come from teaching and research institutions in France or abroad, or from public or private research centers.

L'archive ouverte pluridisciplinaire **HAL**, est destinée au dépôt et à la diffusion de documents scientifiques de niveau recherche, publiés ou non, émanant des établissements d'enseignement et de recherche français ou étrangers, des laboratoires publics ou privés.

**Seasonality and
extent of TST**

P. Hoor et al.

Seasonality and extent of extratropical TST derived from in-situ CO measurements during SPURT

P. Hoor^{1,2}, C. Gurk², D. Brunner¹, M.I. Hegglin¹, H. Wernli^{1,3}, and H. Fischer²

¹Institute for Atmospheric and Climate Science, Swiss Federal Institute of Technology, Zürich, Switzerland

²Max Planck Institute for Chemistry, Air Chemistry, Mainz, Germany

³Institute for Atmospheric Physics, University of Mainz, Germany

Received: 26 January 2004 – Accepted: 17 February 2004 – Published: 16 March 2004

Correspondence to: P. Hoor (peter.hoor@env.ethz.ch)

Title Page

Abstract

Introduction

Conclusions

References

Tables

Figures

◀

▶

◀

▶

Back

Close

Full Screen / Esc

Print Version

Interactive Discussion

© EGU 2004

Abstract

We present airborne in-situ trace gas measurements which were performed on eight campaigns between November 2001 and July 2003 during the SPURT-project (SPURenstofftransport in der Tropopausenregion, trace gas transport in the tropopause region). The measurements on a quasi regular basis allowed an overview on the seasonal variations of the trace gas distribution in the tropopause region over Europe from 35°–75° N to investigate the influence of transport and mixing across the extratropical tropopause on the lowermost stratosphere.

From the correlation of CO and O₃ irreversible mixing of tropospheric air into the lowermost stratosphere is identified. The CO distribution indicates that transport and subsequent mixing of tropospheric air across the extratropical tropopause predominantly affects a layer, which closely follows the shape of the local tropopause. In addition the seasonal cycle of CO₂ illustrates the strong coupling of that layer to the extratropical troposphere. Both, horizontal gradients of CO on isentropes as well as the CO-O₃-distribution in the lowermost stratosphere reveal that the influence of quasi-horizontal transport and subsequent mixing weakens with distance from the local tropopause.

However, at large distances from the tropopause a significant influence of tropospheric air is still evident. The relation between N₂O and CO₂ indicates that a significant contribution of air originating from the tropical tropopause contributes to the background air in the extratropical lowermost stratosphere.

1. Introduction

Mixing of tropospheric air across the extratropical tropopause plays an important role for the trace gas composition in the lowermost stratosphere affecting chemistry and radiative transfer in the UT/LS region at mid and high latitudes. Tropospheric pollutants like volatile organic compounds (VOC's) and reactive nitrogen affect local chemistry in the lowermost stratosphere, thereby acting in particular on the budgets of HO_x and

Seasonality and extent of TST

P. Hoor et al.

Title Page

Abstract

Introduction

Conclusions

References

Tables

Figures

◀

▶

◀

▶

Back

Close

Full Screen / Esc

Print Version

Interactive Discussion

**Seasonality and
extent of TST**

P. Hoor et al.

Title Page

Abstract

Introduction

Conclusions

References

Tables

Figures

◀

▶

◀

▶

Back

Close

Full Screen / Esc

Print Version

Interactive Discussion

© EGU 2004

O₃. Photochemical production of O₃ (Lacis et al., 1990) and mixing of infrared active species originating from the troposphere have direct impact on the radiation budget and therefore on the temperature distribution in the lowermost stratosphere. In particular trends of O₃ in that region are subject of large uncertainties due to the high variability of the underlying photochemical and dynamical processes (WMO, 2003). Therefore, a detailed understanding of extratropical cross tropopause transport and its effect on the trace gas composition is essential to understand the processes controlling photochemistry in the lowermost stratosphere.

It is well known that tropospheric air enters the stratosphere predominantly in the tropics where air is lifted upwards and polewards on timescales of several years taking part in the Brewer-Dobson circulation (Holton et al., 1995). Diabatic downward motion occurs at mid- and high latitudes exhibiting a seasonal cycle. Downward flux through the $\Theta = 380$ K surface maximizes during winter (Appenzeller et al., 1996) contributing to the trace gas composition of the lowermost stratosphere. According to Hoskins (1991) the lowermost stratosphere is defined as the region where isentropes cross the extratropical tropopause, thus enabling bidirectional exchange between both parts of the middleworld (Holton et al., 1995).

In the following we will use the terms TST for troposphere-to-stratosphere transport, STT for stratosphere-to-troposphere transport, both characterizing the transfer of mass across the tropopause (Stohl et al., 2003) associated with a change of PV in the transported air parcel. The latter is a prerequisite for mixing. We will use the term mixing when we refer to an irreversible intermediate chemical composition of the involved air masses. STE (stratosphere-troposphere exchange) refers to the bidirectional process.

Numerous in-situ measurements in the vicinity of tropopause folds confirmed that the tropopause in the extratropics is not totally impermeable to transport and that STE occurs (e.g. Danielsen, 1968; Shapiro, 1980; Kritz et al., 1991). In addition convection has been identified injecting boundary layer air directly into the lowermost stratosphere within several hours (Poulida et al., 1996; Fischer et al., 2003). Radiative processes associated with the decay of anticyclones also might play an important role for TST in

the extratropics (Zierl and Wirth, 1997).

Beside these case studies the results of Dessler et al. (1995) and later Fischer et al. (2000) and Hoor et al. (2002) indicated that the sum of these rather localized TST-processes result in the formation of a mixing layer in the lowermost stratosphere exhibiting the photochemical characteristic of both, the troposphere and the stratosphere.

Model studies indicated only a weak seasonality of the strength of TST on global scales (Sprenger and Wernli, 2003) in contrast to STT. During summer the location of TST shifts to higher isentropic surfaces (Chen, 1995) exhibiting a secondary maximum at $\Theta = 360$ K (Sprenger and Wernli, 2003) possibly due to weaker PV-gradients and therefore a reduced barrier to TST at the subtropical jet (Chen, 1995; Haynes and Shuckburgh, 2000).

Beside the seasonality it is still an open question how far the effect of TST and subsequent mixing extends into the lowermost stratosphere in the vertical (cross isentropic) as well as in the quasi-horizontal direction on isentropes. In the stratosphere the air masses associated with TST furthermore interact with the diabatic downward motion (James et al., 2003).

In-situ measurements addressing this question were limited by their temporal and spatial coverage. Ray et al. (1999) concluded from three balloon profiles at 34.5° N and 64° N, respectively, that the late spring lowermost stratosphere was dominated by air, which descended from $\Theta > 380$ K, whereas in September tropospheric air contributed to a fraction of 50–80%. They concluded that the tropospheric fraction was mixed across the extratropical tropopause into the lowermost stratosphere. Based on two airborne measurement campaigns in Winter 1997 (northern Europe, 69° N) and summer 1998 (Canada, 48° N) Hoor et al. (2002) concluded that mixing across the extratropical tropopause results in the formation of a layer with higher vertical extent in summer than in winter.

The next section gives a short description of the SPURT project and the measurement concept followed by an overview on the experimental setup. After a description of the data coverage in the tropopause region we discuss exemplary CO-profiles and

Seasonality and extent of TST

P. Hoor et al.

Title Page

Abstract

Introduction

Conclusions

References

Tables

Figures

◀

▶

◀

▶

Back

Close

Full Screen / Esc

Print Version

Interactive Discussion

investigate implications for TST in the UT/LS region using the whole SPURT data set. Finally, we will focus on the tropospheric contribution to the stratospheric background air using long-lived tracers like CO₂ and N₂O.

2. Project Overview

5 2.1. The SPURT concept

In 2001 the SPURT (trace gas transport in the tropopause region) project started to investigate dynamical and chemical processes affecting the chemical composition of the extratropical lowermost stratosphere. Although the investigation of TST was the prime focus of the project, single case studies of transport and mixing processes were
10 a minor component of the project. Instead, a seasonal overview on the trace gas distribution in the tropopause region over a broad range of latitudes was investigated to conclude on seasonal variations and the integral effect of individual TST-events on the trace gas composition of the lowermost stratosphere. Therefore, a total of eight airborne measurement campaigns were performed in different months between 2001
15 and 2003. Home base was Hohn (northern Germany, 52° N, 8° E). A typical campaign consisted of a northbound and southbound flights covering a latitude range from approximately 35° N to 75° N (Fig. 1). The flights were performed on two consecutive days and sampled a snapshot of the trace gas distribution in the tropopause region over Europe for a given meteorological situation. Flight planning for each campaign was based
20 on the meteorological forecast provided by the ETH Zürich using operational ECMWF-data. In particular the PV-fields were used to deduce the location of the tropopause for the planning of the individual flights.

Each flight typically consisted of two long flight legs at constant altitude, one leg within the tropopause region and the second one high above in the lowermost strato-
25 sphere. At the end of each flight the aircraft climbed to maximum altitude in order to sample undisturbed stratospheric background air followed by a slow descent providing

Seasonality and extent of TST

P. Hoor et al.

Title Page

Abstract

Introduction

Conclusions

References

Tables

Figures

◀

▶

◀

▶

Back

Close

Full Screen / Esc

Print Version

Interactive Discussion

**Seasonality and
extent of TST**

P. Hoor et al.

Title Page

Abstract

Introduction

Conclusions

References

Tables

Figures

◀

▶

◀

▶

Back

Close

Full Screen / Esc

Print Version

Interactive Discussion

© EGU 2004

high resolution vertical profiles. Intermediate landings were made close to the most southerly and northerly points resulting in a total of eight vertical profiles per campaign at different latitudes. The successive flight on the same day mirrored the flight pattern such that each point along the flight path was sampled at two different altitudes, which was not always possible due to aircraft limitations and air traffic restrictions.

2.2. Experimental setup

A Lear Jet 35 operated by GFD (Gesellschaft für Flugzieldarstellung) in cooperation with the company *enviscope* was used as measurement platform. The aircraft is capable of reaching a maximum flight altitude of 13.7 km and has a range of approximately 2000 km at a cruising speed of 150 m/s. Table 1 gives an overview on the payload and lists the measured species and the used techniques. The trace gas measurements were supplemented by measurements of meteorological parameters such as pressure, temperature and horizontal winds.

CO, CH₄ and N₂O were measured with the Tunable Diode Laser Absorption Spectrometer (TDLAS) TRISTAR (Tracer in situ TDLAS for atmospheric research) (Wienhold et al., 1998; Kormann et al., 2002). Time multiplexing is achieved by pneumatically driven pop-up mirrors allowing subsequent measurement of each species with an integration time of 1.5 s. The time resolution is ultimately limited by the summed integration times for the three measurement channels resulting in a duty cycle of less than 5 s for each species. The instrument is calibrated in-flight using secondary standards of dried ambient air, whose concentrations are cross-calibrated prior to and after the campaigns against a laboratory long term standard. To guarantee consistency over the different campaigns the long term laboratory standard is traced to NOAA standards. The total uncertainty for N₂O, CO and CH₄ is better than 1%, 1.5% and 2.5%, respectively. These values have to be taken as upper limits since the precision is determined from the reproducibility of the in-flight calibrations, thus mainly mirroring the slow drifts of the instrument sensitivity, which are accounted for in the subsequent data processing. Furthermore, N₂O is measured independently by the in-situ GC GHOST (University of

Frankfurt/Main). Both techniques yield an excellent agreement of 98% (H. Bönisch, personal communication).

A LICOR 6262 was used to determine CO₂ mixing ratios with a time resolution of 1 Hz. A constant-pressure inlet allows to operate the instrument at a pressure of 850 (±0.1) hPa. The instrument temperature was stabilized to 40.0°C. Ambient CO₂ is determined against a reference gas of known CO₂ concentration. In-flight calibrations are performed with two secondary standards of compressed dried air, bracketing the expected ambient values. The standards are cross-calibrated against two NOAA CMDL primary standards. Total uncertainty of the measurements is better than 0.1%.

Ozone has been measured using a chemiluminescence detector (ECO-Physics SR-790) with an overall accuracy of 5%. The detector has been calibrated before and after each measurement campaign using a commercial ozone calibrator.

Meteorological forecasts and analysis data were provided by the ETH-Zürich and were based on the 3-h operational ECMWF data with a vertical resolution of 60 levels corresponding to a height resolution of about 700 m at the extratropical tropopause. The meteorological post-flight analysis included the calculation of ten-day backward trajectories (Wernli and Davies, 1997) which were initialized every ten seconds along the flight track, providing information in particular on the history of PV and Θ of the encountered air masses.

3. Data coverage

As mentioned earlier, the main focus of SPURT was to establish an overview of the chemical composition in the tropopause region. For this purpose a sufficient data coverage is crucial. Figure 2 displays the total observation time binned with respect to potential temperature Θ and latitude for all eight campaigns. Superimposed is the tropopause-potential temperature (denoted Θ_{TP} in the following) interpolated along the flight path. Although it was not possible to completely cover the region above the local tropopause, a dense coverage was achieved from 35–75° N up to $\Theta = 360$ K. Two

Seasonality and extent of TST

P. Hoor et al.

Title Page

Abstract

Introduction

Conclusions

References

Tables

Figures

◀

▶

◀

▶

Back

Close

Full Screen / Esc

Print Version

Interactive Discussion

flights to Iceland during SPURT 4 in August 2002 and SPURT 5 in October 2002 resulted in a smaller latitude range for these missions.

The data, which were sampled during each individual measurement campaign covered a broad range of meteorological situations due to meridional northward advection of (sub-)tropical tropospheric air or southward excursions of stratospheric air, both associated with large variations of the tropopause altitude along the flight path. A detailed description of the meteorological situation during each individual flight is beyond the scope of this study and will be given in a separate article. Here, we focus on the temporal and spatial distribution of trace gases in the tropopause region to deduce the extent of TST in the lowermost stratosphere.

The trace gas composition of a single air parcel can be regarded as the sum of several independent individual mixing events and thus represents a spectrum of different air masses and mixing time scales. Therefore a detailed analysis of the meteorological situation during each individual flight is not essential for the understanding of the trace gas distribution in the lowermost stratosphere. However, knowledge of the geographical location of the local tropopause relative to the location of the measurements is crucial to separate tropospheric and stratospheric air.

For the following analysis we used a dynamical definition of the tropopause based on a value of 2 PVU. Although the tropopause was crossed at different Θ -levels several times during each campaign, an in-situ, tracer- or temperature-based tropopause definition is not feasible since the aircraft flew most of the times in varying distances above or below the tropopause. During each campaign at least the $\Theta = 370$ K isentropic surface was crossed generally high above the local tropopause, allowing the characterization of stratospheric air far from recent extratropical tropospheric influence, but close to the lower boundary of the overworld.

Seasonality and
extent of TST

P. Hoor et al.

Title Page

Abstract

Introduction

Conclusions

References

Tables

Figures

◀

▶

◀

▶

Back

Close

Full Screen / Esc

Print Version

Interactive Discussion

4. Results

4.1. Irreversibility of TST

To identify TST and subsequent mixing across the extratropical tropopause we used the relation between CO and O₃. The most important source for CO in the stratosphere is the photochemical degradation of CH₄ via OH. Destruction of CO takes place via the reaction with OH forming CO₂ resulting in a lifetime of CO on the order of several months. If no additional CO from the troposphere is mixed into the stratosphere, a steady state volume mixing ratio of 8–15 ppbv establishes which is the balance between photochemical production from CH₄ and the much faster CO oxidation via OH (Flocke et al., 1999). High altitude measurements by the ER-2 in the tropics as well as in polar regions indicated almost constant CO-values of 12 ppbv (Flocke et al., 1999; Toon et al., 1999). Closer to the local tropopause in general increasing values are observed reflecting transport of tropospheric air into the stratosphere. Thus, in the stratosphere any excess CO above the equilibrium level indicates a contribution of air of tropospheric origin.

In a CO-O₃ scatter-plot mixing of air across the tropopause leads to the formation of mixing lines connecting stratospheric background and upper tropospheric CO- and O₃-values, respectively. In particular, the appearance of mixing lines associated with an intermediate photochemical composition of air in the lowermost stratosphere indicates the irreversibility of the mixing process. The method is described in detail in Fischer et al. (2000) and Hoor et al. (2002).

Figure 3 displays the CO-O₃-scatterplot for the campaign in February 2003. A rather compact anticorrelation covering almost the entire range of stratospheric O₃-mixing ratios is evident. Just above the tropopause O₃ mixing ratios between 100–300 ppbv accompanied by CO values ranging from 40–75 ppbv indicate a mixture of tropospheric and stratospheric air. A close inspection reveals distinct mixing lines indicating mixing from recent TST-events of various tropospheric origins. Different CO concentrations in the upper troposphere, which are involved in these mixing events result in the observed

Seasonality and extent of TST

P. Hoor et al.

Title Page

Abstract

Introduction

Conclusions

References

Tables

Figures

◀

▶

◀

▶

Back

Close

Full Screen / Esc

Print Version

Interactive Discussion

**Seasonality and
extent of TST**P. Hoor et al.

[Title Page](#)[Abstract](#)[Introduction](#)[Conclusions](#)[References](#)[Tables](#)[Figures](#)[◀](#)[▶](#)[◀](#)[▶](#)[Back](#)[Close](#)[Full Screen / Esc](#)[Print Version](#)[Interactive Discussion](#)

© EGU 2004

different slopes of the individual mixing lines. However, most points form the broad compact central band which can be regarded as the sum of individual mixing events which are already completed and possibly remixed thereby forming a 'smoothed' mean slope. This major part of the correlation is therefore independent from the current meteorological situation which on the other hand may determine individual mixing lines.

Higher up in the lowermost stratosphere at ozone levels exceeding 300 ppbv, the slope of the anticorrelation becomes steeper and less scattered, indicating a layer with different air mass characteristics. In particular individual mixing lines that connect directly to the local tropopause are absent despite the large data coverage during SPURT 6 (comp. Fig. 2). Note that TST and subsequent mixing associated even with a small amount of tropospheric air would appear as mixing line in such a scatter plot as long as mixing is incomplete.

The absence of mixing lines above $O_3 > 300$ ppbv and the steep and compact anticorrelation indicate that recent injections from the extratropical troposphere are of minor importance in this part of the stratosphere. Nevertheless, tropospheric influence is still evident due to the fact that observed CO-values ranging from 20–45 ppbv significantly exceed the stratospheric equilibrium value. The rather sharp transition between these two layers in the lowermost stratosphere indicates two regions with a different degree of tropospheric influence, different air mass histories and possibly mixing time scales.

4.2. Trace gas profiles and vertical structure of the lowermost stratosphere

Figure 4a shows the whole CO-dataset which was obtained from the five mission flights during SPURT 6 using Θ as vertical coordinate. The tropopause altitude along the flight tracks during this campaign varied between 350 hPa and 200 hPa corresponding to variations in Θ_{TP} from 295–335 K (compare Fig. 2). A large part of the scatter in Fig. 4a is due to this variation of the tropopause potential temperature Θ_{TP} . In particular no significant upper or lower boundary for tropospheric influence becomes evident.

The picture changes significantly, if potential temperature relative to the local

tropopause is used as vertical coordinate ($\Delta\Theta$ [K]). $\Delta\Theta$ was deduced from ECMWF-data by calculating the difference between Θ and Θ_{TP} at the position of the aircraft along the flight path. We used the potential temperature difference $\Delta\Theta$ as a measure for the vertical distance from the instantaneous local tropopause.

In Fig. 4b the CO data from SPURT 6 are shown as a function of $\Delta\Theta$ instead of Θ . The profile exhibits less scatter resulting in a much higher compactness. In contrast to Fig. 4a the vertical distribution now displays a kink at $\Delta\Theta = 25$ K separating two regimes of different chemical composition within the lowermost stratosphere. Just above the local tropopause CO decreases rapidly within a layer of $\Delta\Theta = 25$ K from tropospheric values down to mixing ratios of less than 45 ppbv. At greater vertical distances from the tropopause the decrease of CO is much more gradual leading to a steeper CO gradient than directly above the tropopause.

The change of gradient in the vertical CO-profile which appears at $\Delta\Theta = 25$ K corresponds to a mean CO value of 45 ppbv. Note that the kink in the CO-O₃ scatter plot (Fig. 3) is evident at the same CO value separating photochemically aged air and a layer which is influenced by recent mixing as indicated by distinct mixing lines in Fig. 3. Thus, the respective region between the local tropopause and $\Delta\Theta < 25$ K (Fig. 4b) is strongly influenced by recent TST-events and subsequent mixing at the extratropical tropopause. It is interesting to note that the overall effect of different individual processes and events exhibits a common upper boundary, although the data were collected over a broad latitude range (35°–85° N) and variations of Θ_{TP} from 295 K–335 K.

A similar behaviour can also be identified from other trace gas measurements. For example, CO₂ exhibits almost the same vertical distribution relative to $\Delta\Theta$ (Fig. 4c) including a sharp transition at $\Delta\Theta = 25$ K. Since CO₂ has no photochemical sinks in the lowermost stratosphere its distribution is exclusively controlled by dynamics. It is thus unlikely that the structure seen in the CO-distribution was caused predominantly by photochemical degradation associated with a longer residence time in this part of the lowermost stratosphere. Instead, the sharp change of gradient of the CO- and CO₂-profiles at $\Delta\Theta = 25$ K separates air masses with different fractions of tropospheric air,

**Seasonality and
extent of TST**

P. Hoor et al.

Title Page

Abstract

Introduction

Conclusions

References

Tables

Figures

◀

▶

◀

▶

Back

Close

Full Screen / Esc

Print Version

Interactive Discussion

**Seasonality and
extent of TST**

P. Hoor et al.

Title Page

Abstract

Introduction

Conclusions

References

Tables

Figures

I◀

▶I

◀

▶

Back

Close

Full Screen / Esc

Print Version

Interactive Discussion

© EGU 2004

thus different histories, within the lowermost stratosphere. This rather well pronounced separation in the lowermost stratosphere marked by the 'kink' in the vertical CO- and CO₂-ΔΘ profiles (Fig. 4b and Fig. 4c) and the CO-O₃-correlation (Fig. 3) was found during all campaigns independent of season or latitude.

5 The most compact relationships appeared between CO and ΔΘ (Table 2). We used Spearman's rank correlation to compare the correlation between CO and the respective parameters since it is independent of the 'shape' of the distribution. Thus we don't have to make any assumptions on the functional relationship between CO and the respective parameters. Although the definition of ΔΘ is based on PV (PV = 2 PVU)
10 a stronger correlation between CO and ΔΘ than for CO and PV is found. On the one hand Θ is determined from in-situ measurements of pressure and temperature whereas PV is calculated on a coarse grid. On the other hand PV-gradients might determine trace gas distributions rather than absolute values of PV. The fact that the highest degree of correlation appears between ΔΘ and CO implies that the CO-distribution
15 in the lowermost stratosphere is more dependent on the vertical distance from the local tropopause than on the absolute Θ-value of the isentropic surface. This has consequences for the extent of the TST-impact in the lowermost stratosphere which will be discussed in the next section.

5. Discussion

20 5.1. Seasonal variation of the mixing layer

To investigate the horizontal extent of the TST-impact along isentropic surfaces we used the Θ-equivalent latitude coordinate system. Equivalent latitude ϕ_{eq} can be obtained by transforming the area that is enclosed by a PV-contour on a given isentrope to a pole-centered circle of equal area. The distance of the respective PV-circles from the
25 equator in degrees latitude represents ϕ_{eq} , forming a unique relation between PV and ϕ_{eq} on each isentropic surface. The ϕ_{eq} -Θ-coordinate system can be regarded as

**Seasonality and
extent of TST**

P. Hoor et al.

Title Page

Abstract

Introduction

Conclusions

References

Tables

Figures

◀

▶

◀

▶

Back

Close

Full Screen / Esc

Print Version

Interactive Discussion

© EGU 2004

5 tropopause-following since it follows the meridional excursions of PV-contours induced by planetary waves. Using a value of $PV = 2$ PVU (associated to a unique ϕ_{eq}) for the extratropical tropopause, trace gas mixing ratios, which are displayed in this coordinate system, therefore appear according to their distance to the local tropopause on a given isentropic surface. For SPURT PV- ϕ_{eq} -relations have been calculated for 37 individual isentropes from $\Theta = 270$ –400 K in steps of 5 K. The equivalent latitude of each measurement point then was obtained by bilinear interpolation from the discrete $\phi_{eq}(PV, \Theta)$ -distribution to the PV- and Θ -values at the observation.

10 Figure 5 shows the distribution of CO for the whole set of SPURT missions mapped onto ϕ_{eq} - Θ -coordinates. In the troposphere CO exhibits significant latitudinal gradients in agreement with the climatology of CO for the northern hemisphere (e.g. Emmons et al., 2000; Novelli et al., 1992). The strongest decline of CO mixing ratios is observed in a layer from $PV = 2$ –6 PVU (black lines), where CO decreases from tropospheric values down to less than 50 ppbv. Thus, the CO-isopleths in the low-
15 ermost stratosphere are non-parallel to isentropes resulting in a tropopause-following layer structure independent from season. As stated in the previous section, these CO mixing ratios from 50–80 ppbv indicate a mixture of tropospheric and stratospheric air. Moreover, the existence of a tropopause-following layer implies that the effect of mixing out of this layer further into the lowermost stratosphere is only weak or the processes are slow since CO-gradients extend along isentropes further into the lowermost strato-
20 sphere.

25 In Fig. 5 the stratospheric end points of those ten-day backward trajectories are superimposed, which indicate TST (black dots) and ended along the flight path. We selected only TST-trajectories which stayed for at least 24 hrs before and after crossing the tropopause in the troposphere and stratosphere, respectively. If quasi-horizontal mixing of tropospheric air deep into the lowermost stratosphere were fast, one could expect a large spread of TST trajectories on isentropic surfaces. However, this is not observed. Almost all TST-trajectories end in close vicinity to the local tropopause below 6 PVU and $\Delta\Theta < 20$ K. The distribution of TST as indicated by the TST-trajectories

roughly matches the distribution of regions with elevated CO in the stratosphere and supports the hypothesis that TST and subsequent mixing in along isentropes on short time scales mainly affects a layer close to the local tropopause.

The picture deduced from the absolute CO volume mixing ratio might be biased by the seasonal and latitudinal variations of CO in the troposphere. From Fig. 5 it is difficult to deduce a seasonality of the extent of mixing or to conclude on variations of the layer depth. Therefore, we normalized CO to its value in the upper troposphere ($\Delta\Theta > -5$ K, $PV < 2$ PVU, CO_{UT}) on isentropic surfaces intersecting the tropopause. Since we had no observations of CO at the tropopause for equivalent latitudes south of 35° N we interpolated CO along the tropopause to CO mixing ratios of 55 ppbv at $\Theta = 380$ K according to the climatology of Herman et al. (1999). We assumed a background equilibrium value of 12 ppbv (referred to as CO_{bkgd}) being representative for undisturbed stratospheric air. The resulting tropospheric CO-fraction $CO_{TS} = (CO - CO_{bkgd}) / (CO_{UT} - CO_{bkgd})$ should be independent of the seasonal and latitudinal variations of tropospheric CO-values, and thus reflect predominantly the effect of TST and mixing on time scales of days to weeks.

Note, that the fraction CO_{TS} without any additional information is not equal to the mass fraction of tropospheric air in the lowermost stratosphere due to the limited photochemical lifetime of CO of the order of three months. In the stratosphere the CO mixing ratio of an air parcel is not only determined by mixing but also by photochemical degradation depending on the time since last contact to the troposphere. Thus, the approach provides a lower limit for the fraction of tropospheric air in the lowermost stratosphere since photochemical degradation of CO is not accounted for.

The distribution of the CO_{TS} in $\phi_{eq} - \Delta\Theta$ -coordinates (Fig. 6) confirms the conclusions which are drawn from the absolute CO volume mixing ratios in Fig. 5. The large enhancements in November 2001 result from a southbound flight in the vicinity of a deep stratospheric intrusion adjacent to a tropospheric ridge with $\Theta_{TP} > 360$ K (see Fig. 2) and an almost vertical dynamical tropopause, indicative for a tropopause break. Since $\Delta\Theta$ is defined as the vertical distance from the $PV = 2$ PVU-surface a vertical

**Seasonality and
extent of TST**P. Hoor et al.

Title Page

Abstract

Introduction

Conclusions

References

Tables

Figures

◀

▶

◀

▶

Back

Close

Full Screen / Esc

Print Version

Interactive Discussion

**Seasonality and
extent of TST**

P. Hoor et al.

Title Page

Abstract

Introduction

Conclusions

References

Tables

Figures

◀

▶

◀

▶

Back

Close

Full Screen / Esc

Print Version

Interactive Discussion

© EGU 2004

tropopause results in very large $\Delta\Theta$ -values (compare SPURT 1 in Fig. 5 and Fig. 6). The system was associated with a strong jet as well as convective activity ahead of the surface cold front. A detailed case study by Hegglin et al. (2003) suggests that this convective activity over the southwestern Mediterranean, which was associated with intense lightning activity, was responsible for the injection of significant amounts of NO_y and water vapor into the lowermost stratosphere.

The use of $\Delta\Theta$ instead of Θ in Fig. 6 illustrates that isolines of constant tropospheric fraction roughly follow the tropopause ($\Delta\Theta = 0$). A ratio of $\text{CO}_{\text{TST}} = 40\%$ approximates the 1/e-photochemical lifetime (37%) which we use as a measure for extratropical TST and subsequent mixing within the CO-lifetime. With the exception of the outstanding SPURT 1-campaign the distributions for the corresponding seasons over different years show similar patterns. Largest layer depths and variabilities of the tropospheric fraction are observed during the summer campaigns. During the rest of the year a rather homogenous layer structure was found rarely exceeding $\Delta\Theta = 20$ K. In case of homogenous CO-distributions on isentropic surfaces one would expect an increasing layer depth at higher ϕ_{eq} due to the sloping tropopause on isentropic surfaces (comp. Fig. 5). Instead, rather constant mixing layer depths in terms of $\Delta\Theta$ [K] or even increasing layer depths towards low latitudes are observed (SPURT 1, SPURT 4, SPURT 8). In Fig. 6 the stratospheric end points of TST-trajectories are again superimposed. The trajectories indeed correspond to air parcels showing an enhanced tropospheric CO-fraction. In particular during SPURT 1 and SPURT 4 CO_{TST} and TST-trajectories both indicate significant TST within the last 10 days. Note the large vertical spread of trajectory-indicated TST during summer in agreement with a higher mixing layer depths deduced from the tropospheric CO-fraction.

A larger depth of the summer mixing layer is in agreement with the seasonal cycle found in theoretical studies (Chen, 1995; Haynes and Shuckburgh, 2000) and the measurement-based conclusions by Hoor et al. (2002). Moreover, during summer a stronger tropospheric contribution is indicated towards lower equivalent latitudes being in close agreement with an additional maximum for TST near $\Theta = 360$ K (Sprenger

and Wernli, 2003). In contrast, during winter diabatic downward transport from the overworld maximizes (Appenzeller et al., 1996) leading to a stronger contribution of overworld air filling the lowermost stratosphere with aged CO-depleted air during late winter/spring.

5 Therefore, we conclude that only the lowest $\Delta\Theta = 20$ K (30 K during summer) above the tropopause are influenced by TST and subsequent mixing with extratropical tropospheric air on time scales of days to a few weeks.

5.2. Beyond the mixing layer

10 Beyond the mixing layer above the tropopause CO mixing ratios higher than the undisturbed stratospheric CO-equilibrium value indicate that the air cannot be regarded as purely stratospheric from a photochemical point of view. In this part of the lower stratosphere either time scales for mixing have to be longer, allowing CO to be photochemically processed, or the amount of tropospheric air reaching these distances from the tropopause is smaller. To address mixing processes exceeding the CO-lifetime we used
15 relations between long-lived tracers like N_2O with a photochemical lifetime of 100 years and CO_2 which is virtually inert in the lower stratosphere.

CO_2 with its well known tropospheric seasonal cycle provides useful informations on the transit time scale and the tropospheric origin of the mixed air masses. In Fig. 7 upper tropospheric CO_2 ($\Delta\Theta = -20-0$ K) shows a strong seasonal cycle with a spring-time maximum in May 2002 and April 2003, respectively. The minimum is found during
20 summer which is in accordance with measurements of Nakazawa et al. (1991). Just above the tropopause at ($\Delta\Theta = 0-20$ K) the same seasonal pattern is evident which confirms the strong coupling between the lowermost stratosphere and the extratropical troposphere through TST and subsequent mixing in accordance with the analysis in the previous section. The dampening of the amplitude of the seasonal cycle reflects
25 the role of the extratropical tropopause as a barrier to transport. Above $\Delta\Theta = 20$ K the phase maximum is shifted towards summer. The delay of three months indicates a phase lag due to longer transit times for the tropospheric fraction of air, which is mixed

Seasonality and
extent of TST

P. Hoor et al.

Title Page

Abstract

Introduction

Conclusions

References

Tables

Figures

◀

▶

◀

▶

Back

Close

Full Screen / Esc

Print Version

Interactive Discussion

into the lowermost stratosphere, and possibly a different transport path.

To investigate if isentropic mixing delayed by three months can account for the observed phase lag in the lowermost stratosphere, we evaluated the seasonal cycle of CO₂ on isentropic surfaces (Fig. 7b). Similar to Fig. 7a a clear phase shift is evident between $\Theta = 320$ K and 360 K. At $\Theta = 340$ K no distinct minima or maxima occur due to averaging the CO₂ seasonal cycles from the mixing layer ($\Delta\Theta < 20$ K) and the lower stratospheric background ($\Delta\Theta > 20$ K). The isentropic view reveals that isentropic mixing from the extratropics cannot account for the observed phase signal. The CO₂-maximum which is found above $\Theta = 360$ K in August 2002 exceeds any value which was measured during the preceding campaigns in the same layer. Therefore it cannot be regarded as a remnant of isentropic cross tropopause mixing during the previous months. Similarly local cross isentropic transport from tropospheric altitudes (e.g. through convection) cannot account for the phase maximum at the highest isentropic surfaces observed in August 2002 due to the negative vertical CO₂-gradient during summer.

If TST and subsequent mixing in the extratropics cannot account for the tropospheric fraction of air in the lowermost stratosphere, the air most likely entered the stratosphere at the tropical tropopause. To find a tropical signature in our data we analyzed the correlation between CO₂ and N₂O. Both species are longlived enough to obey the conditions for slope equilibrium (Plumb and Ko, 1992) i.e. their isopleths are controlled by dynamics as opposed to photochemistry. We evaluated the correlation for $\Delta\Theta > 45$ K to exclude recent TST and mixing from the extratropics, but to have a statistically significant data base (300–1100 data points per campaign). Following Hintsä et al. (1999) we applied a liner fit to the reduced N₂O-CO₂-relationship and extrapolated the tropospheric end member of CO₂ assuming a tropopause value of 317 ppbv for N₂O (WMO, 2003). The applied fit method accounts for the uncertainties in both measurements (Press et al., 1999) and returns the standard deviation of the parameters.

Figure 8 displays the deduced tropospheric CO₂ end members for the SPURT-campaigns as well as the average of the surface data of Samoa and Mauna Loa

**Seasonality and
extent of TST**

P. Hoor et al.

Title Page

Abstract

Introduction

Conclusions

References

Tables

Figures

◀

▶

◀

▶

Back

Close

Full Screen / Esc

Print Version

Interactive Discussion

**Seasonality and
extent of TST**

P. Hoor et al.

Title Page

Abstract

Introduction

Conclusions

References

Tables

Figures

◀

▶

◀

▶

Back

Close

Full Screen / Esc

Print Version

Interactive Discussion

© EGU 2004

(Keeling and Whorf, 2003). We found that a backward timeshift of 2.5 months gave the best agreement between the extrapolated tropical SPURT CO₂ tropopause values and the averaged surface cycles. Andrews et al. (1999) showed that at $\Theta = 390$ K the maximum of the seasonal cycle occurs in early July in agreement with observations of Boering et al. (1996) who used a delay of two months for the propagation of the surface signal to these altitudes. Since the phase maximum occurs around mid of June in the tropical troposphere (Nakazawa et al., 1991; Matsueda and Inoue, 1996) the air most likely entered the tropical stratosphere at $\Theta = 380$ K between mid of June and the beginning of July resulting in a horizontal transport time to high latitudes of about one month which is in close agreement with Boering et al. (1996).

The large error bar for the summer campaign is the result of a data base of only 300 points and a large scatter of the data resulting in a poor correlation coefficient. For the spring missions in May 2002 (SPURT 3) and April 2003 (SPURT 7), respectively, a time lag of 2.5 months is too short to match the tropical seasonal cycle. The extrapolated CO₂ tropopause values from SPURT indicate a longer transient time since tropospheric entry. Most likely the springtime lowermost stratosphere carries a larger contribution of aged air from higher altitudes which descended from $\Theta > 380$ K. The net downward mass transport across the 380 K isentropic surface maximizes during winter (Appenzeller et al., 1996) leading to an increasing fraction of photochemically aged air in late winter and spring in the lowermost stratosphere. Thus, the contribution of air masses with a longer transit time since last contact with the tropical tropopause is larger than during the rest of the year.

Ray et al. (1999) stated that the lowermost stratosphere is more strongly influenced by air descending from above $\Theta > 380$ K during springtime than at the end of summer. Our results show a similar pattern, however we can identify a significant contribution of air originating from the tropical tropopause in the extratropical lowermost stratosphere. Ray et al. (1999) addressed the tropospheric influence in their data to mixing across the extratropical tropopause, which is no applicable explanation for the propagation of the seasonal CO₂-cycle on different isentropic surfaces which is observed during SPURT.

**Seasonality and
extent of TST**

P. Hoor et al.

Title Page

Abstract

Introduction

Conclusions

References

Tables

Figures

◀

▶

◀

▶

Back

Close

Full Screen / Esc

Print Version

Interactive Discussion

© EGU 2004

Therefore, we conclude that the lowermost stratosphere above $\Delta\Theta = 30$ K is significantly affected by tropospheric air, which entered the stratosphere at the tropical tropopause. According to Rosenlof et al. (1997) these air masses are partly transported quasi horizontally to mid- and high latitudes within 2–4 months where they mix with photochemically aged air which diabatically descends from the overworld. Grewe et al. (2002) calculated transport timescales of not more than 1.5 months for tropical tropospheric air being transported to the extratropical lowermost stratosphere. In agreement with observations Andrews et al. (2001) found, that stratospheric CO_2 time series (for $\text{N}_2\text{O} > 255$ ppbv) are represented best by bimodal age spectra consisting of a young peak of less than one year and a broad peak representing aged air of the order of 4–5 years. Diabatic descent (Appenzeller et al., 1996) from $\Theta > 380$ K leads to the observed tropical contribution of air in the lowermost stratospheric background far from the extratropical tropopause. Closer to the extratropical tropopause the phase shift of CO_2 between $\Delta\Theta < 20$ K and $\Delta\Theta > 20$ K suggests, that TST and mixing in the extratropics dominates over the diabatically descending tropical tropospheric fraction of air.

6. Conclusions

The extensive data set obtained during the SPURT missions facilitated a broad overview of the seasonal distribution of trace gases over Europe. The CO distribution in the lowermost stratosphere indicates the existence of a mixing layer which establishes above the local tropopause. The mixing layer exhibits trace gas signatures being characteristic for a mixture of young tropospheric and stratospheric air. The depth of the layer exhibits a weak seasonal cycle showing the largest elevation of $\Delta\Theta = 30$ K above the local tropopause in summer and 20–25 K during the rest of the year. The seasonal cycle of CO_2 in the mixing layer shows the same phase as in the troposphere illustrating the strong coupling between both regions. Within the lowermost stratosphere the influence of TST and subsequent mixing decreases with distance from the local

**Seasonality and
extent of TST**

P. Hoor et al.

Title Page

Abstract

Introduction

Conclusions

References

Tables

Figures

◀

▶

◀

▶

Back

Close

Full Screen / Esc

Print Version

Interactive Discussion

© EGU 2004

tropopause in both vertical and horizontal direction resulting in a mixing layer which closely follows the local tropopause. Based on ER-2 measurements of CO and O₃ Pan et al. (2003) suggested to view the extratropical tropopause as a layer characterized by intermediate tracer mixing ratios due to rapid and shallow exchange (Stohl et al., 2003). Similar conclusions based on trajectory calculations have been drawn from James et al. (2003) showing that layers of the same age are a function of distance to the tropopause and not of isentropic surfaces in agreement with the observed CO isopleths during SPURT.

At larger distances from the local tropopause the CO₂ phase lag as well as CO values exceeding the stratospheric steady state mixing ratio both indicate tropospheric influence, but on different transient- and mixing time scales. From the relationship between CO₂ and N₂O and tropical surface data we could determine an average transport time of 2.5 months from the tropics to the extratropical lowermost stratosphere above $\Theta = 370$ K. Due to the strong downwelling in the extratropics during winter the contribution of overworld air is enhanced in accordance with Ray et al. (1999).

Acknowledgements. Without the excellent support by the company GFD (Gesellschaft für Flugzieldarstellung) in cooperation with the company enviscope in operating the Lear Jet the whole SPURT project would not have been possible. We are grateful to the German Ministry for Education and Research for financial support within the AFO-2000 programme and to the Swiss National Fond.

Edited by: A. Stohl

References

Andrews, A. E., Boering, K. A., Wofsy, S. C., Daube, B. C., Hints, E. J., Weinstock, E. M., and Bui, T. P.: Empirical age spectra for the lower tropical stratosphere from in situ observations of CO₂: Implications for stratospheric transport, *J. Geophys. Res.*, 104, 26 581–26 595, 1999. 1708

**Seasonality and
extent of TST**

P. Hoor et al.

Title Page

Abstract

Introduction

Conclusions

References

Tables

Figures

◀

▶

◀

▶

Back

Close

Full Screen / Esc

Print Version

Interactive Discussion

© EGU 2004

- Andrews, A. E., Boering, K. A., Wofsy, S. C., Daube, B. C., Jones, D. B., Alex, S., Loewenstein, M., Podolske, J. R., and Strahan, S. E.: Empirical age spectra for the midlatitude lower stratosphere from in-situ observations of CO₂: Quantitative evidence for a subtropical “barrier” to horizontal transport, *J. Geophys. Res.*, 106, 10 257–10 274, 2001. [1709](#)
- Appenzeller, C., Holton, J. R., and Rosenlof, K. H.: Seasonal variation of mass transport across the tropopause, *J. Geophys. Res.*, 101, 15 071–15 078, 1996. [1693](#), [1706](#), [1708](#), [1709](#)
- Boering, K. A., Wofsy, S. C., Daube, B. C., Schneider, J. R., Loewenstein, M., Podolske, J. R., and Conway, T. J.: Stratospheric mean ages and transport rates from observations of CO₂ and N₂O, *Science*, 274, 1340–1343, 1996. [1708](#)
- Chen, P.: Isentropic cross tropopause mass exchange in the extratropics, *J. Geophys. Res.*, 100, 16 661–16 673, 1995. [1694](#), [1705](#)
- Danielsen, E. F.: Stratospheric-tropospheric exchange based upon radioactivity, ozone, and potential vorticity, *J. Atmos. Sci.*, 25, 502–518, 1968. [1693](#)
- Dessler, A. E., Hints, E. J., Weinstock, E. M., Anderson, J. G., and Chan, K. R.: Mechanism controlling water vapor in the lower stratosphere: “A tale of two stratospheres”, *J. Geophys. Res.*, 100, 23 167–23 172, 1995. [1694](#)
- Emmons, L. K., Hauglustaine, D. A., Müller, J.-F., Carrol, M. A., Brasseur, G. P., Brunner, D., Staehelin, J., Thourét, V., and Marengo, A.: Data composites of airborne observations of tropospheric ozone and its precursors, *J. Geophys. Res.*, 105, 20 497–20 538, 2000. [1703](#)
- Fischer, H., Wienhold, F. G., Hoor, P., Bujok, O., Schiller, C., Siegmund, P., Ambaum, M., Scheeren, H. A., and Lelieveld, J.: Tracer correlations in the northern high latitude lowermost stratosphere: Influence of cross-tropopause mass exchange, *Geophys. Res. Lett.*, 27, 97–100, 2000. [1694](#), [1699](#)
- Fischer, H., de Reus, M., Traub, M., Williams, J., Lelieveld, J., de Gouw, J., Warneke, C., Schlager, H., Minikin, A., Scheele, R., and Siegmund, P.: Deep convective injection of boundary layer air into the lowermost stratosphere at midlatitudes, *Atmos. Chem. Phys.*, 3, 739–745, 2003. [1693](#)
- Flocke, F., Herman, R. L., Salawitch, R. J., Atlas, E., Webster, C. R., Schauffler, S. M., Lueb, R. A., May, R. D., Moyer, E. J., Rosenlof, K. H., Scott, D. C., Blake, D. R., and Bui, T. P.: An examination of chemistry and transport processes in the tropical lower stratosphere using observations of long-lived and short-lived compounds obtained during STRAT and POLARIS, *J. Geophys. Res.*, 104, 26 625–26 642, 1999. [1699](#)
- Grewe, V., Reithmeier, C., and D., S.: Dynamic-chemical coupling of the upper troposphere

and lower stratosphere region, Chemosphere: Global Change Science, 47, 851–861, 2002.

1709

Haynes, P. and Shuckburgh, E.: Effective diffusivity as a diagnostic of atmospheric transport, 2., Troposphere and lower stratosphere, J. Geophys. Res., 105, 22 795–22 810, 2000. [1694](#),

1705

5 Hegglin, M. I., Brunner, D., Wernli, H., Schwierz, C., Martius, O., Krebsbach, M., Schiller, C., Spelten, N., Hoor, P., Fischer, H., Parchatka, U., Weers, U., Staehelin, J., and Peter, T.: Tracing troposphere to stratosphere transport within a mid-latitude deep convective system, Atmos. Chem. Phys. Discuss., 105, 22 795–22 810, 2003. [1705](#)

Herman, R. L., Webster, C. R., May, R. D., Scott, D. C., Hu, H., Moyer, E. J., Wennberg, P. O., Hanisco, T. F., Lanzendorf, E. J., Salawitch, R. J., Yung, Y. L., Margitan, J. J., and Bui, T. P.: Measurements of CO in the upper troposphere and lower stratosphere, Chemosphere: Global Change Science, 1, 173–183, 1999. [1704](#)

15 Hintsä, E. J., Boering, K. A., Weinstock, E. M., Anderson, J. G., Gary, B. L., Pfister, L., Daube, B. C., Wofsy, S. C., Loewenstein, M., Podolske, J. R., Margitan, J. J., and Bui, T. P.: Troposphere-to-stratosphere transport in the lowermost stratosphere from measurements of H₂O, CO₂, N₂O and O₃, Geophys. Res. Lett., 25, 2655–2658, 1999. [1707](#)

Holton, J. R., Haynes, P. H., McIntyre, M. E., Douglass, A. R., Rood, R. B., and Pfister, L.: Stratosphere-troposphere exchange, Rev. Geoph., 33, 403–439, 1995. [1693](#)

20 Hoor, P., Fischer, H., Lange, L., Lelieveld, J., and Brunner, D.: Seasonal variations of a mixing layer in the lowermost stratosphere as identified by the CO-O₃ correlation from in situ measurements, J. Geophys. Res., 107, 4044, doi:10.1029/2000JD000289, 2002. [1694](#), [1699](#), [1705](#)

Hoskins, B. J.: Towards a PV- θ -view of the general circulation, Tellus, Ser. A/B, 43, 27–35, 1991. [1693](#)

25 James, P., Stohl, A., Forster, C., Eckhardt, S., Seibert, P., and Frank, A.: A 15-year climatology of stratosphere-troposphere exchange with a Lagrangian particle dispersion model: 1. Methodology and validation, J. Geophys. Res., 108, doi:10.1029/2002JD002637, 2003. [1694](#), [1710](#)

30 Keeling, C. D. and Whorf, T. P.: Atmospheric CO₂ records from sites in the SIO air sampling network, Carbon Dioxide Information Analysis Center, Oak Ridge National Laboratory, U.S. Department of Energy, Oak Ridge, Tenn., USA, 2003. [1708](#)

Kormann, R., Fischer, H., Gurk, C., Helleis, F., Klüpfel, T., Kowalski, K., Königstedt, R., Par-

ACPD

4, 1691–1726, 2004

Seasonality and extent of TST

P. Hoor et al.

Title Page

Abstract

Introduction

Conclusions

References

Tables

Figures

◀

▶

◀

▶

Back

Close

Full Screen / Esc

Print Version

Interactive Discussion

© EGU 2004

**Seasonality and
extent of TST**

P. Hoor et al.

Title Page

Abstract

Introduction

Conclusions

References

Tables

Figures

◀

▶

◀

▶

Back

Close

Full Screen / Esc

Print Version

Interactive Discussion

© EGU 2004

chatka, U., and Wagner, V.: Application of a multi-laser tunable diode laser absorption spectrometer for atmospheric trace gas measurements at sub-ppbv levels, *Spectrochim. Acta A*, 58, 2489–2498, 2002. [1696](#)

Kritz, M. A., Rosner, S. W., Danielsen, E. F., and Selkirk, H. B.: Air mass origins and troposphere to stratosphere exchange associated with mid-latitude cyclogenesis and tropopause folding inferred from ^7Be measurements, *J. Geophys. Res.*, 96, 17 405–17 414, 1991. [1693](#)

Lacis, A. A., Wuebbles, D. J., and Logan, J. A.: Radiative forcing of climate by changes in the vertical distribution of ozone, *J. Geophys. Res.*, 95, 9971–9981, 1990. [1693](#)

Matsueda, H. and Inoue, H.: Measurements of atmospheric CO_2 and CH_4 using a commercial airliner from 1993 to 1994, *Atmos. Environ.*, 30, 1647–1655, 1996. [1708](#)

Nakazawa, T., Miyashita, K., Aoki, S., and Tanaka, M.: Temporal and spatial variations of upper tropospheric and lower stratospheric carbon dioxide, *Tellus*, 43B, 106–117, 1991. [1706](#), [1708](#)

Novelli, P. C., Steele, L. P., and Tans, P. P.: Mixing ratios of carbon monoxide in the troposphere, *J. Geophys. Res.*, 97, 20 731–20 750, 1992. [1703](#)

Pan, L., Randel, W., Browell, E., Gary, B., Mahoney, M., and Hints, E.: Definitions and sharpness of the extratropical tropopause: A trace gas perspective, submitted to *J. Geophys. Res.*, 2003. [1710](#)

Plumb, R. A. and Ko, M. K. W.: Interrelationships between mixing ratios of long-lived stratospheric constituents, *J. Geophys. Res.*, 97, 10 145–10 156, 1992. [1707](#)

Poulida, O., Dickerson, R. R., and Heymsfield, A.: Stratosphere-troposphere exchange in a mid latitude mesoscale convective complex, 1. Observations, *J. Geophys. Res.*, 101, 6823–6836, 1996. [1693](#)

Press, W. H., Vetterling, W., Teukolsky, S., and Flannery, B.: Numerical recipes in Fortran 77: The art of scientific computing, Cambridge University Press, 2 edn., 1999. [1707](#)

Ray, E. A., Moore, F. L., Elkins, J. W., Dutton, G. S., Fahey, D. W., Vömel, H., Oltmans, S. J., and Rosenlof, K. H.: Transport into the Northern Hemisphere lowermost stratosphere revealed by in situ tracer measurements, *J. Geophys. Res.*, 104, 26 565–26 580, 1999. [1694](#), [1708](#), [1710](#)

Rosenlof, K. H., Tuck, A. F., Kelly, K. K., Russel, J. M., and McCormick, M. P.: Hemispheric asymmetries in water vapor and inferences about transport in the lower stratosphere, *J. Geophys. Res.*, 102, 13 213–13 234, 1997. [1709](#)

Shapiro, M. A.: Turbulent mixing within tropopause folds as a mechanism for the exchange of

chemical constituents between the stratosphere and troposphere, *J. Atmos. Sci.*, 37, 994–1004, 1980. [1693](#)

Sprenger, M. and Wernli, H.: A northern hemispheric climatology of cross-tropopause exchange for the ERA15 time period (1979–1993), *J. Geophys. Res.*, 108, doi:10.1029/2002JD002636, 2003. [1694](#), [1705](#)

5 Stohl, A., Wernli, H., James, P., Bourqui, M., Forster, C., Liniger, M. A., Seibert, P., and Sprenger, M.: A new perspective of stratosphere-troposphere exchange, *Bull. Am. Met. Soc.*, 84, 1565–1573, 2003. [1693](#), [1710](#)

Toon, G. C., Blavier, J.-F., Sen, B., Margitan, J. J., Webster, C. R., Max, R. D., Fahey, D. W., Gao, R., DelNegro, L., Proffitt, M., Elkins, J., Romashkin, P. A., Hurst, D. F., Oltmans, S., Atlas, E., Schauffler, S., Flocke, F., Bui, T. P., Stimpfle, R. M., Bonne, G. P., Voss, P. B., and Cohen, R. C.: Comparison of MkIV balloon and ER-2 aircraft measurements of atmospheric trace gases, *J. Geophys. Res.*, 104, 26 779–26 790, 1999. [1699](#)

Wernli, H. and Davies, H. C.: A Lagrangian based analysis of extratropical cyclones, 1, The method and some applications, *Q. J. R. Meteorol. Soc.*, 123, 467–489, 1997. [1697](#)

Wienhold, F., Fischer, H., Hoor, P., Wagner, V., Königstedt, R., Harris, G., Anders, J., Grisar, R., Knothe, M., Riedel, W., Lübken, F., and T., S.: TRISTAR – a tracer in situ TDLAS for atmospheric research, *App. Phys. B-Lasers and Optics*, 67, 411–417, 1998. [1696](#)

WMO: Scientific assessment of ozone depletion: 2002, Global Ozone Research and Monitoring Project, Report No. 47, World Meteorological Organization, 2003. [1693](#), [1707](#)

Zierl, B. and Wirth, V.: The role of radiation for stratosphere-troposphere exchange in an upper tropospheric anticyclone, *J. Geophys. Res.*, 102, 23 883–23 894, 1997. [1694](#)

**Seasonality and
extent of TST**

P. Hoor et al.

Title Page

Abstract

Introduction

Conclusions

References

Tables

Figures

◀

▶

◀

▶

Back

Close

Full Screen / Esc

Print Version

Interactive Discussion

Seasonality and extent of TST

P. Hoor et al.

Table 1. Instrumentation during SPURT.

species	technique	institute
CO, N ₂ O, CH ₄	TDLAS	MPI Mainz
CO ₂	NDIR (LiCor-6262)	MPI Mainz
NO, NO _y , O ₃	CLD + gold converter	ETH Zürich
H ₂ O	Lyman- α -fluorescence	FZ Jülich
O ₃	UV-absorption	FZ Jülich
N ₂ O, F-12, SF ₆	in-situ GC	University Frankfurt/Main

[Title Page](#)
[Abstract](#)
[Introduction](#)
[Conclusions](#)
[References](#)
[Tables](#)
[Figures](#)
[Back](#)
[Close](#)
[Full Screen / Esc](#)
[Print Version](#)
[Interactive Discussion](#)

Seasonality and extent of TST

P. Hoor et al.

Table 2. Statistical dependencies for the profiles of CO versus Θ , $\Delta\Theta$ and PV during SPURT.

campaign	date	Spearman's ρ : CO vs.		
		Θ	$\Delta\Theta$	PV
SPURT 1, NOV	10.–11.11.2001	-0.71	-0.85	-0.91
SPURT 2, JAN	17.–19.01.2002	-0.85	-0.94	-0.89
SPURT 3, MAY	16.–17.05.2002	-0.88	-0.94	-0.90
SPURT 4, AUG	22.–23.08.2002	-0.80	-0.89	-0.85
SPURT 5, OCT	17.–18.10.2002	-0.75	-0.89	-0.79
SPURT 6, FEB	16.–17.02.2003	-0.80	-0.87	-0.74
SPURT 7, APR	26.–27.04.2003	-0.89	-0.94	-0.84
SPURT 8, JUL	09.–10.07.2003	-0.75	-0.87	-0.78

[Title Page](#)
[Abstract](#)
[Introduction](#)
[Conclusions](#)
[References](#)
[Tables](#)
[Figures](#)
[Back](#)
[Close](#)
[Full Screen / Esc](#)
[Print Version](#)
[Interactive Discussion](#)

Seasonality and extent of TST

P. Hoor et al.

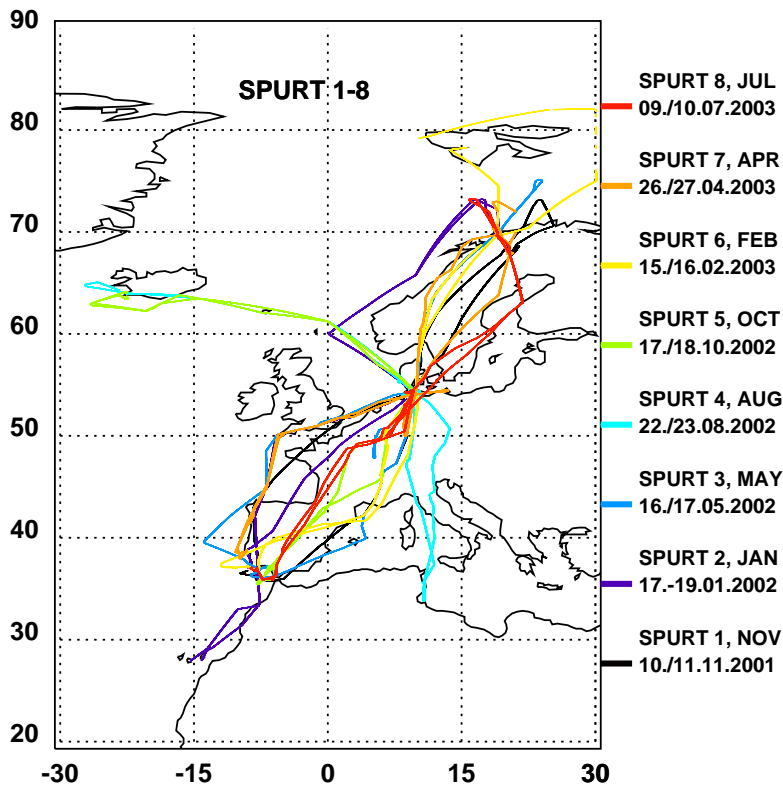


Fig. 1. Flight tracks for the SPURT missions from November 2001 to July 2003.

Title Page

Abstract Introduction

Conclusions References

Tables Figures

◀ ▶

◀ ▶

Back Close

Full Screen / Esc

Print Version

Interactive Discussion

Seasonality and
extent of TST

P. Hoor et al.

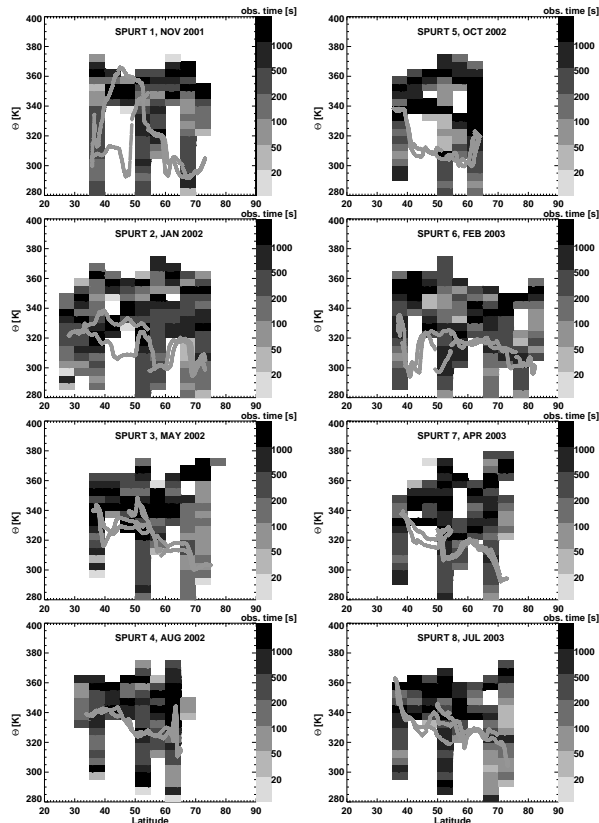


Fig. 2. Data coverage for SPURT as a function of latitude and theta. The location of the local tropopause at the position of the aircraft is superimposed. Note the variability of potential temperature at the tropopause during each deployment.

[Title Page](#)[Abstract](#)[Introduction](#)[Conclusions](#)[References](#)[Tables](#)[Figures](#)[◀](#)[▶](#)[◀](#)[▶](#)[Back](#)[Close](#)[Full Screen / Esc](#)[Print Version](#)[Interactive Discussion](#)

© EGU 2004

**Seasonality and
extent of TST**

P. Hoor et al.

Title Page

Abstract

Introduction

Conclusions

References

Tables

Figures

◀

▶

◀

▶

Back

Close

Full Screen / Esc

Print Version

Interactive Discussion

© EGU 2004

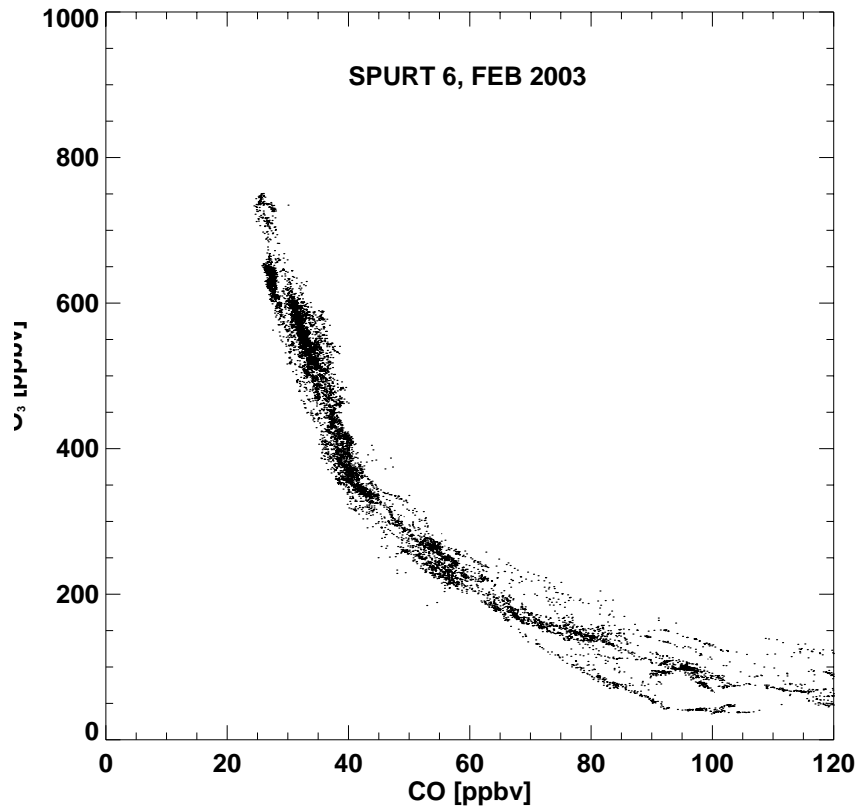


Fig. 3. Scatterplot of CO and ozone for SPURT 6 in February 2003. Taking an ozone threshold of 100 ppbv as an approximation for the tropopause the anticorrelation indicates irreversible cross tropopause mixing. Note, that at $O_3 = 300$ ppbv the slope abruptly changes indicating a rather sharp transition between different layers.

Seasonality and
extent of TST

P. Hoor et al.

Title Page

Abstract

Introduction

Conclusions

References

Tables

Figures

◀

▶

◀

▶

Back

Close

Full Screen / Esc

Print Version

Interactive Discussion

© EGU 2004

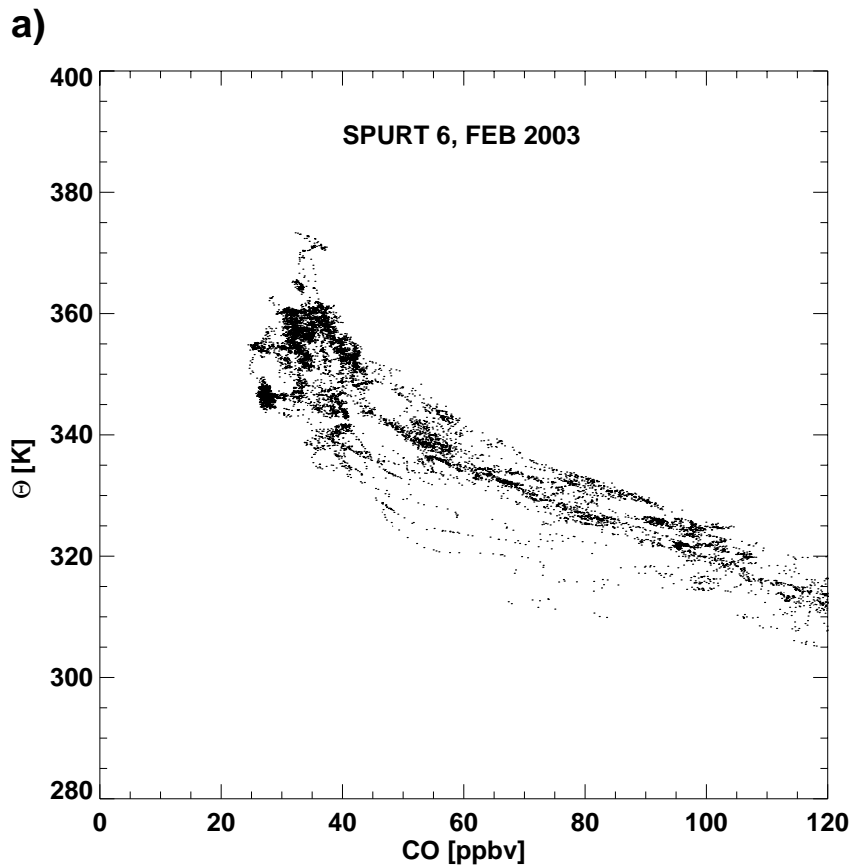


Fig. 4. (a) Complete CO data set obtained during the SPURT 6 missions as a function of (a) potential temperature and (b) potential temperature relative to the local tropopause $\Delta\Theta$. Note the more compact $\Delta\Theta$ -profile and the rather sharp change of the CO gradient at $\Delta\Theta = 25$ K. (c) CO_2 as a function of $\Delta\Theta$ during SPURT 6 showing the same behaviour at $\Delta\Theta = 25$ K.

**Seasonality and
extent of TST**

P. Hoor et al.

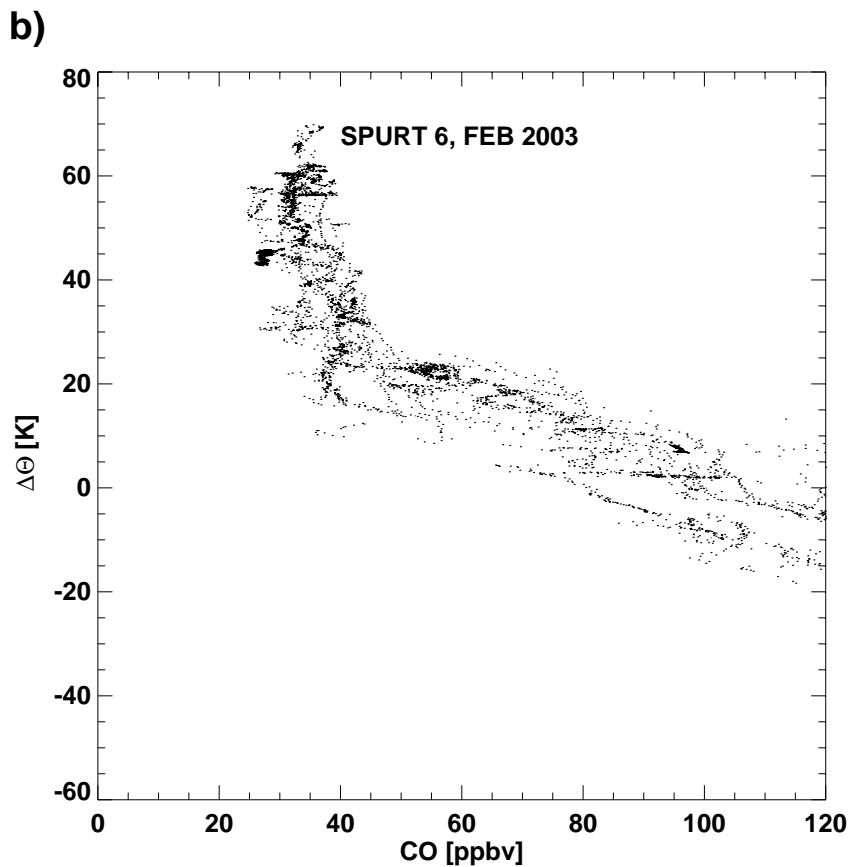


Fig. 4. Continued.

[Title Page](#)[Abstract](#)[Introduction](#)[Conclusions](#)[References](#)[Tables](#)[Figures](#)[I◀](#)[▶I](#)[◀](#)[▶](#)[Back](#)[Close](#)[Full Screen / Esc](#)[Print Version](#)[Interactive Discussion](#)

© EGU 2004

**Seasonality and
extent of TST**

P. Hoor et al.

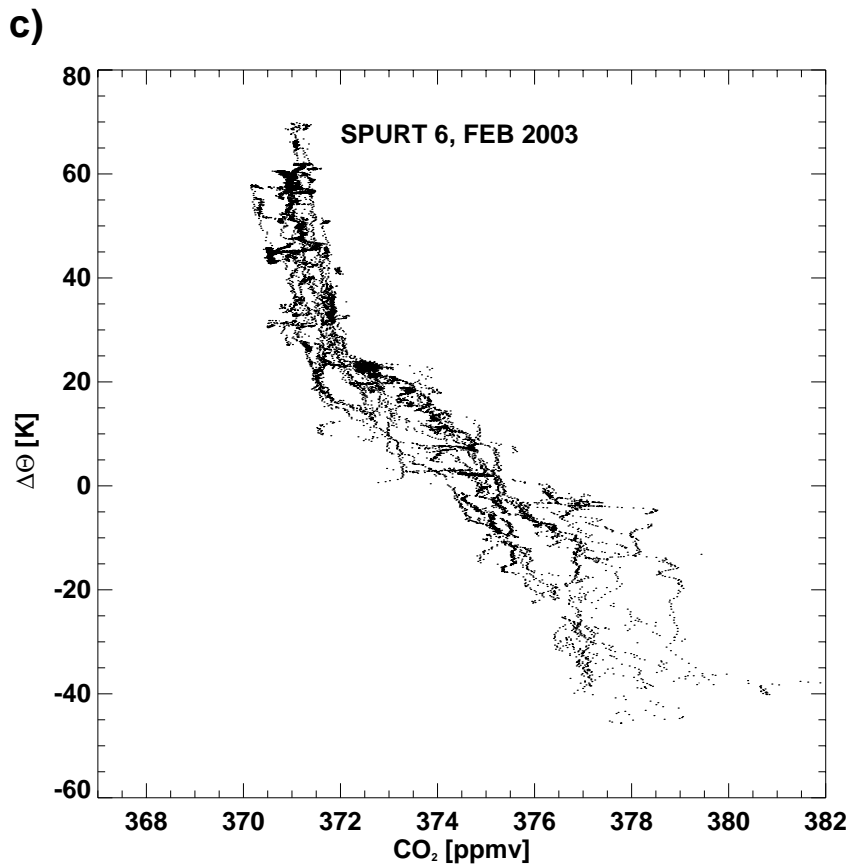


Fig. 4. Continued.

[Title Page](#)[Abstract](#)[Introduction](#)[Conclusions](#)[References](#)[Tables](#)[Figures](#)[I◀](#)[▶I](#)[◀](#)[▶](#)[Back](#)[Close](#)[Full Screen / Esc](#)[Print Version](#)[Interactive Discussion](#)

© EGU 2004

Seasonality and
extent of TST

P. Hoor et al.

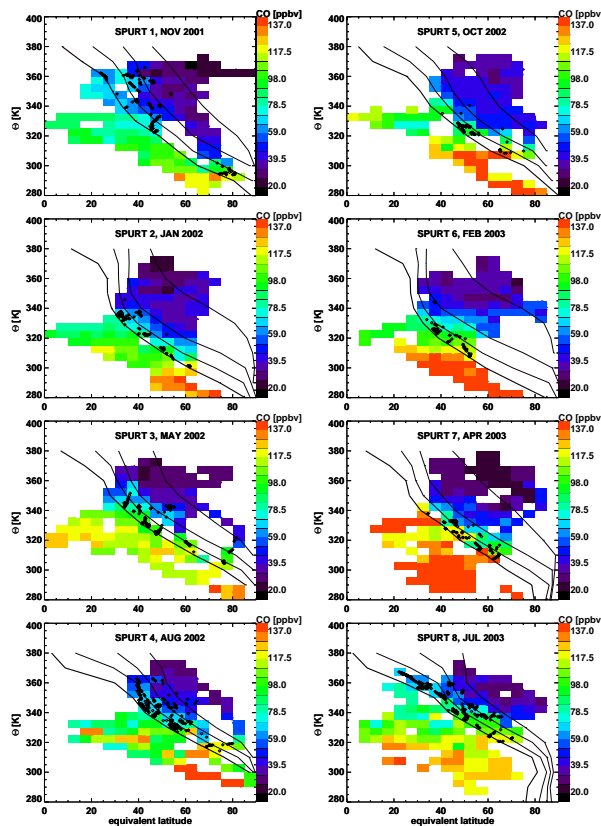


Fig. 5. CO-distribution in equivalent latitude ϕ_{eq} - Θ -coordinates for the whole SPURT-deployment. The thick black line denotes the location of the tropopause $PV = 2$ PVU-surface, thin lines mark the 4,6 and 8 PVU-contours, respectively. Superimposed are the positions of 10-day backward trajectories indicating TST within ten days before the flights.

Title Page

Abstract

Introduction

Conclusions

References

Tables

Figures

◀

▶

◀

▶

Back

Close

Full Screen / Esc

Print Version

Interactive Discussion

© EGU 2004

Seasonality and
extent of TST

P. Hoor et al.

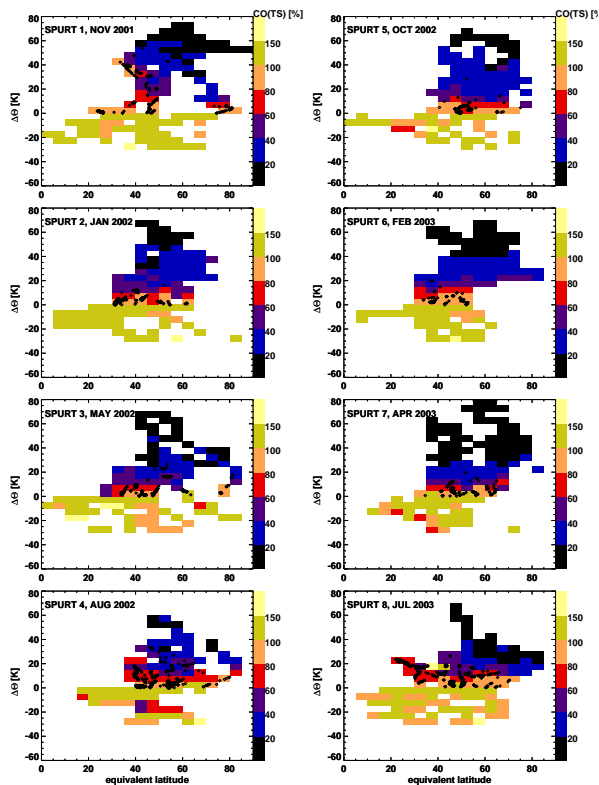


Fig. 6. Tropospheric fraction of CO relative to the respective isentropic tropopause CO-value in Fig. 5 as a function of equivalent latitude and $\Delta\Theta$ above the tropopause (details see text).

[Title Page](#)[Abstract](#)[Introduction](#)[Conclusions](#)[References](#)[Tables](#)[Figures](#)[◀](#)[▶](#)[◀](#)[▶](#)[Back](#)[Close](#)[Full Screen / Esc](#)[Print Version](#)[Interactive Discussion](#)

© EGU 2004

Seasonality and
extent of TST

P. Hoor et al.

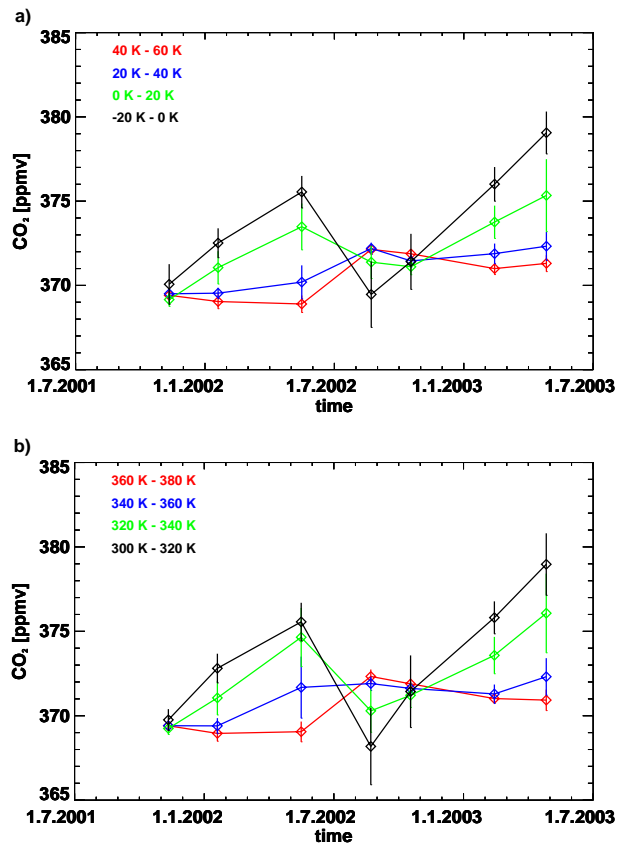


Fig. 7. (a) CO₂ as a function of time and $\Delta\Theta$ above the local tropopause. The phase shift at $\Delta\Theta > 20$ K is evident. (b) CO₂ on isentropic surfaces. Note the local maximum in summer on the highest isentropic surface of $\Theta = 360$ K and the negative vertical CO₂ gradient in August 2002.

[Title Page](#)[Abstract](#)[Introduction](#)[Conclusions](#)[References](#)[Tables](#)[Figures](#)[◀](#)[▶](#)[◀](#)[▶](#)[Back](#)[Close](#)[Full Screen / Esc](#)[Print Version](#)[Interactive Discussion](#)

© EGU 2004

Seasonality and
extent of TST

P. Hoor et al.

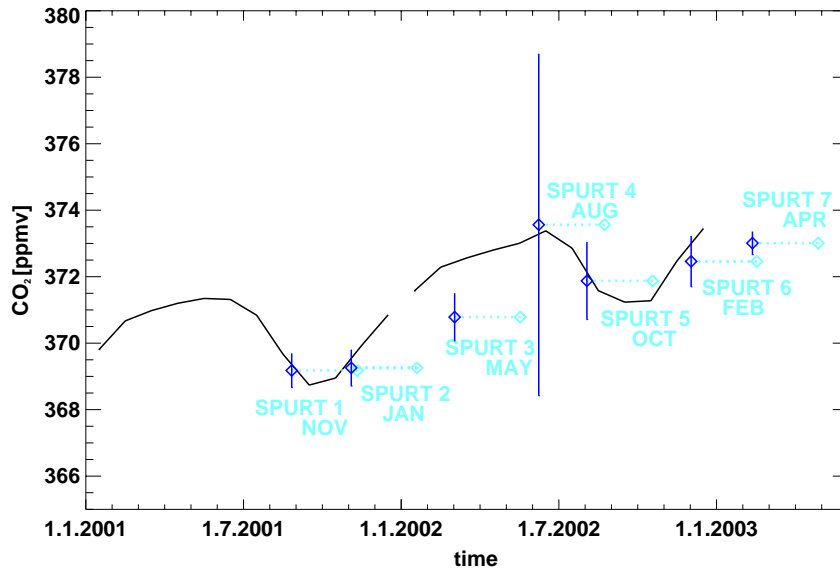


Fig. 8. Tropical CO₂ surface data and tropical tropopause CO₂-data deduced from SPURT shifted backward in time by 2.5 months (dark blue), light blue: time of measurement. Error bars are deduced from the error of the fit parameters of the N₂O-CO₂-correlation for $\Delta\Theta > 45$ K (details see text).

[Title Page](#)[Abstract](#)[Introduction](#)[Conclusions](#)[References](#)[Tables](#)[Figures](#)[◀](#)[▶](#)[◀](#)[▶](#)[Back](#)[Close](#)[Full Screen / Esc](#)[Print Version](#)[Interactive Discussion](#)

© EGU 2004